

Effects of climatic variability on the thermal properties of Lake Washington

George B. Arhonditsis^{1,2} and Michael T. Brett

Department of Civil and Environmental Engineering, Box 352700, University of Washington, Seattle, Washington, 98195

Curtis L. DeGasperis

King County Department of Natural Resources and Parks, Wastewater Treatment Division, 201 South Jackson Street, MS KSC-NR-0512, Seattle, Washington, 98104-3854

Daniel E. Schindler

Department of Biology, University of Washington, 404 Kincaid Hall, Box 351800, Seattle, Washington, 98195

Abstract

We conducted a statistical analysis of a long-term (1964–1998) record of intra- and interannual temperature fluctuations in Lake Washington, Washington. Lake Washington has experienced a warming trend, with overall increases of 1.5 (0.045°C yr⁻¹) and 0.9°C (0.026°C yr⁻¹), respectively, for temperature data weighted over the surface (0–10 m) and entire lake volume. This warming trend was greatest for the period from April to September and was smallest and nonsignificant for November–February. A principal-components analysis of the long-term mean monthly temperature time series identified two independent modes of interannual variability. The first mode represented the months of the year when the lake warms and is warmest (e.g., March–October) and explained 54% of the variability in the overall time series. The second mode represented the months when the lake cools and is coldest (November–February) and explained 24% of the variability. The March–October mode was positively correlated with interannual variability in air temperatures and the Pacific Decadal Oscillation (PDO), multivariate $r^2 = 0.65$. The November–February mode was positively correlated with air temperature, PDO, relative humidity, solar radiation, and wind speed ($r^2 = 0.83$). A heat budget model indicated that long-term trends had a secondary role and interannual variability dominated, with exceptions being net long-wave atmospheric radiation and surface-emitted radiation, for which the long-term trend explained ~25% and 53% of the total variance, respectively. An increase in incoming long-wave radiation fluxes was mainly associated with the increase in minimum daily temperatures (0.06°C yr⁻¹, $r^2 = 0.47$), especially during the March–October mode, when the linear trend accounted for 85% of the variability.

Climatic and large-scale oceanic fluctuations are increasingly recognized as important regulatory factors that are capable of influencing the structural properties of both terrestrial and aquatic ecosystems (Aebischer et al. 1990; Adrian et al. 1995; George and Taylor 1995; Post et al. 1997; Beamish et al. 1999). Generally, the thermal properties of aquatic ecosystems are more directly governed by these broad-scale phenomena than are the thermal properties of terrestrial ecosystems, with lakes appearing to be particularly sensitive to the ecological impacts of climatic forcing (Hostetler and Small 1999; Gerten and Adrian 2001). There is clear evidence of a strong relationship between climatic conditions (e.g., air temperature and wind patterns) and lake thermal structure (e.g., onset of stratification, thermocline depth, mean epilimnetic temperature, turnover date, and duration of ice cover) for northern temperate lakes (Schindler et al.

1990; King et al. 1997; Livingstone 1999, 2003; George et al. 2000; Livingstone and Dokulil 2001). The influence of these macroscale atmospheric processes and the persistence of their signals varies substantially among lakes with different sizes, thermal structures, and mixing regimes, which indicates different information storage abilities even under similar climatic conditions (Shuter et al. 1983; Gerten and Adrian 2001).

Climate-stimulated biological responses in lakes are an important issue, and several long time series have shown coupling between lake water temperatures and individual organism physiology, population abundance, and community structure. For example, Weyhenmeyer et al.'s (1999) study of Lake Erken in Sweden showed the North Atlantic Oscillation has a stronger statistical association with the timing and composition of the spring phytoplankton bloom than do local parameters (such as ice break-up and nutrient concentrations). Straile (2000) found a complex interplay among meteorological, hydrological, and ecological processes induced temporal shifts in successional events for the Lake Constance planktonic community that persisted for 6 months. In contrast, Gerten and Adrian (2000) observed short-memory climatic effects. These authors also suggested that a basic knowledge of the relationships among global climate indices, local meteorological conditions, and the thermal response of various lake types is essential in pre-

¹ Corresponding author (georgea@u.washington.edu).

² Present address: Nicholas School of the Environment and Earth Sciences, Duke University, Durham, North Carolina.

Acknowledgments

We thank two anonymous reviewers for very helpful comments regarding the manuscript.

This study was supported by a grant from the King County, Department of Natural Resources and Parks, Wastewater Treatment Division. Support from the Andrew W. Mellon Foundation funded much of the data collection.

dicting the biological effects of climate change on freshwater ecosystems.

In western North American marine and lacustrine ecosystems, the El Niño–Southern Oscillation (ENSO) (Strub et al. 1985; Goldman et al. 1989; Jassby et al. 1990) and the Pacific Decadal Oscillation (PDO) (Mantua et al. 1997; McGowan et al. 1998) are large-scale meteorological phenomena that can influence thermal structure and biotic community dynamics. For example, in Castle Lake, California, much of the primary production variability observed in June and July was attributed to the ENSO, with the role of ENSO expressed via its impact on winter snowfall and spring rain, which determined the timing of ice out and the intensity of spring hydraulic flushing (Jassby et al. 1990). A clear distinction between the ENSO and PDO is complicated, because these phenomena are spatially and temporally related (Mantua et al. 1997). However, there is no doubt that both interannual (ENSO) and interdecadal (PDO) climatic variation affects the structure and function of North American ecosystems (McGowan et al. 1998), and combining PDO and ENSO information may enhance empirical climatic forecasting in this geographic area (McGabe and Dettinger 1999).

We conducted a statistical analysis of intra- and interannual temperature fluctuations for a long-term (1964–1998) record of Lake Washington, Washington, thermal properties. Our goal was to quantitatively describe interannual variability in the seasonal water temperature dynamics and to detect the underlying drivers of these changes. Conventional climatic parameters (such as air temperature, solar radiation, relative humidity, rainfall, wind speed, and direction) and PDO and ENSO indices were used to decompose the interannual variability in Lake Washington's thermal properties. A heat-budget model was also developed to quantify the contribution of various energy fluxes to the observed lake temperature dynamics, to investigate the mechanisms through which lake-atmosphere interactions were expressed.

Materials and methods

Study site and data description—Lake Washington is the second largest natural lake in Washington state, with a surface area of 87.6 km² and a total volume of 2.9 km³. The mean lake depth is 32.9 m (maximum depth: 65.2 m), the summer epilimnion depth is ~10 m, and the epilimnion: hypolimnion volume ratio during the stratified period averages 0.39. Lake Washington's two largest tributaries are Cedar River (at the south end) and Sammamish River (at the north end), which contribute ~57% and 27%, respectively, of the annual hydraulic load. The hydraulic retention time of the lake averages 2.4 yr (Edmondson and Lehman 1981). The majority of Lake Washington's immediate watershed (1,274 km²) is urbanized, with 63% of the immediate watershed surface area fully developed (Brett et al. unpubl. data).

We used water temperature data collected at weekly to biweekly intervals from a central station off Madison Park from 1964 to 1998. The Madison Park site is the classic Edmondson sampling station and is located at the deepest

point in Lake Washington (Edmondson and Lehman 1981). A mechanical bathythermograph was used from 1964 to 1986, when temperatures were recorded every 1 m for depths above the thermocline and then every 5 m to the bottom below the thermocline. Since 1986, temperature has been recorded with a Kahl digital thermometer every meter, if the temperature changes by at least 0.1°C m⁻¹, down to a depth of 20 m and then every 5 m to the bottom (Edmondson 1997). Hourly mean meteorological data (air temperature, relative humidity, wind speed, wind direction, solar radiation, and rainfall) were available from the SeaTac Airport weather station (47°45'N, 122°30'W; 137 m). Wind data before 1969 were excluded from our analyses because of obvious inconsistencies in annual trends before and after this year that were caused by a change in instrumentation. Therefore, the heat-budget analysis was only for the period 1969–1998. Monthly values for the PDO index were obtained from the Joint Institute for the Study of the Atmosphere and Oceans, University of Washington (http://tao.atmos.washington.edu/data_sets/). This index is defined as the leading principal component of the North Pacific monthly sea surface temperature variability (poleward of 20°N for the 1900–1993 period). ENSO effects were characterized by monthly values for the Multivariate ENSO Index (MEI), which was provided by the Climate Diagnostics Center, National Oceanic and Atmospheric Administration Web site (<http://www.cdc.noaa.gov/~kew/MEI/>). Six variables (sea-level pressure, zonal and meridional components of the surface wind, sea surface temperature, surface air temperature, and total cloudiness fraction of the sky) observed over the tropical Pacific are used when computing the MEI index. After spatially filtering the individual fields into clusters, the MEI is calculated as the first unrotated principal component (PC) for all six fields (Wolter and Timlin 1993). The MEI is computed separately for 12 sliding bimonthly categories (Dec/Jan, Jan/Feb, and Nov/Dec), whereas the PDO is calculated for specific months. Finally, air temperature data for two rural (Snoqualmie Falls and Startup) meteorological stations in the Seattle region (which we used to estimate the urban heat island effect) were obtained from the National Oceanographic and Atmospheric Association National Climatic Data Center's Web site (<http://www.ncdc.noaa.gov/>).

Data aggregation—Water temperature data were binned by month on the basis of time-weighted averages—weekly or biweekly field measurements were linearly interpolated, and the resulting daily time series was averaged over the months. Volume-weighted water temperatures (overall, 0–10 and 10–bottom) were calculated using lake morphometric data (Edmondson and Lehman 1981). Monthly mean climatic variables were also used for these analyses.

Time-series analysis—We extracted seasonal patterns by seasonal-trend decomposition using the X-11 (Census II) method, which is an extension and refinement of the classic seasonal decomposition and adjustment method (Census I) and contains many ad hoc features that allow for a series of successive refinements and adjustments for outliers and extreme values (Kendall and Ord 1990). The time series was separated into three different components—seasonal, trends,

and residual—whereas an additive model was chosen to define their functional relationships. After time-series decomposition, we subtracted the seasonal component (centering the data) and inspected the residual values for nonstationarity problems.

Modes of interannual variability—We applied PC analysis (PCA) to analyze interannual variability in a manner similar to that used in recent studies (e.g., Jassby et al. 2002) and as described in detail by Jassby (1999). The basic rationale behind this application of PCA for time-series decomposition is that different phases of the intra-annual cycle may be regulated by separate processes and may therefore behave independently of each other, thus impeding the development of clear causal statistical models. The significance of PCs was determined using the Monte Carlo technique known as the “rule of N” (Overland and Preisendorfer 1982). Significant PCs were rotated using the normalized varimax strategy (raw factor loadings divided by the square roots of the respective communalities), and the new component coefficients and amplitude time series were calculated (Richman 1986).

We then developed simple and multiple linear regression models between the individual modes of variability and variables representing plausible causal factors. We replaced the resulting modes of variability with the water temperature averages over the corresponding periods, because the amplitude time series and the averaged temperatures were highly correlated ($r^2 = 0.96$ and 0.90 , respectively, for the first and second modes) and because statistical models based on the original data are easier for most users to comprehend because they are in familiar units (Jassby 1999). The best subset of predictor variables in multiple regression models was selected based on Mallows’s criterion, which is a measure of the quality of fit that is less dependent on the number of variables included in the statistical model than are r^2 values. Hence, Mallows’s criterion tends to find the best subset of variables, including only the most important predictors for the respective dependent variables, thereby providing more parsimonious models.

Heat-budget model—We developed a heat-budget model for Lake Washington, to explore the potential physical mechanisms causing the short- and long-term changes in thermal condition observed in this ecosystem. We used a one-dimensional model that simulates the vertical structure of temperature. Because its application was intended to quantify the contribution of various energy fluxes to the observed patterns of the lake temperature dynamics, high-model spatial resolution was deemed to be unnecessary. Hence, we included only two spatial compartments, representing the epilimnion and hypolimnion of the lake. The depths of the two boxes varied with time and were explicitly defined on the basis of field temperature measurements. During the stratified period, the epilimnion was defined as the maximum depth where the water temperature varied $\geq 1^\circ\text{C}$ relative to the temperature at 0.5 m; otherwise, we assumed a box depth of 20 m, to reproduce patterns of incomplete mixing that regulate the ecological processes in the lake during the early

spring (Arhonditsis et al. unpubl.). The two governing equations were

$$\frac{\partial T_{\text{epi}}}{\partial t} = \frac{H_{\text{sn}(0)}A_0 - H_{\text{sn}(z)}A_z(t)}{V_{\text{epi}}(t) \cdot \rho c_p} + \sum_{i=a,n,b,c,e} \frac{H_i A_0}{V_{\text{epi}}(t) \cdot \rho c_p} \pm \frac{1}{V_{\text{epi}}(t)} \left\{ A_z(t) \left[K(t) \frac{\Delta T}{\Delta z} \right] \right\} + f(t) \quad (1)$$

$$\frac{\partial T_{\text{hypo}}}{\partial t} = \frac{H_{\text{sn}(z)}A_z(t)}{V_{\text{hypo}}(t) \cdot \rho c_p} \mp \frac{1}{V_{\text{hypo}}(t)} \left\{ A_z(t) \left[K(t) \frac{\Delta T}{\Delta z} \right] \right\} \quad (2)$$

where T_{epi} and T_{hypo} are the epilimnion and hypolimnion temperature, respectively ($^\circ\text{C}$); V_{epi} and V_{hypo} are the epilimnion and hypolimnion volume, respectively (m^3); ρ is the density of lake water (kg m^{-3}), c_p is the specific heat of lake water ($\text{J kg}^{-1} \text{C}^{-1}$), $K(t)$ is the molecular plus the eddy diffusion coefficients for heat ($\text{m}^2 \text{d}^{-1}$); $f(t)$ is the external heat sources ($^\circ\text{C d}^{-1}$); z is epilimnion depth (m); A_0 and $A_z(t)$ are the area at the surface and depth z , respectively (m^2); $\Delta T/\Delta z$ is the temperature gradient between the centers of the two boxes; and H_{sn} and H_i are the heat fluxes (detailed description below). Values of the vertical diffusion coefficient were based on measurements from past studies of this lake (Walters 1980; Quay et al. 1980). External heat sources in the model were the stream inflows from the surrounding watershed (King County 2002; Brett et al. unpubl. data), whereas heat fluxes between the sediment and water column were assumed to be negligible compared with surface heat exchange and were not taken into account.

The formulations of the heat-exchange processes across the air-water interface, which determine the heat balance of the lake, are presented in Table 1. The net incoming short-wave radiation (H_{sn}), which comes directly from the sun, depends on the altitude of the sun (varies daily and seasonally for a fixed location on the earth) and the dampening effect of scattering and absorption in the atmosphere due to cloud cover and the Earth’s surface albedo. In addition, short-wave radiation can penetrate the water column, and this process was modeled using a light-extinction coefficient K_d that assumed Beer’s Law. K_d values were calculated from the Secchi depth (z_{sd} , m) using the relationship $K_d = 1.7/z_{\text{sd}}$ (Idso and Gilbert 1974). The net long-wave radiation (H_{an}) emitted by the atmosphere (the so-called thermal infrared radiation) primarily depends on air temperature, humidity, cloud cover, and cloud height. It is also affected by ozone, carbon dioxide, and possibly other materials in the atmosphere, which were not included in the present model. The third source of radiation transfer through the air-water interface is surface-emitted long-wave radiation from the lake surface (H_b). The remaining two mechanisms are linked to matter and represent heat transfer between the water and the atmosphere caused by temperature differences (sensible heat fluxes H_c -conduction/convection) or water vapor exchange (latent heat fluxes H_e -evaporation/condensation). The difference between conduction and convection is that the former represents the transfer of heat from molecule to molecule when matter of different temperatures comes in contact (analogous to diffusive transport), and convection is asso-

Table 1. Heat budget for Lake Washington. Equations and parameters describing heat transfer across the air–water interface.

Process	Expressions	Definitions
Net short-wave solar radiation (H_{sn})	$H_{sn} = H_s(1 - R_s)(1 - 0.63C_L^2)$	C_L : Cloudiness as the decimal fraction of the sky covered
Extraterrestrial radiation (H_o)	$H_s = H_o\tau_a + \tau_b H_o$ $H_o = \frac{24 \times 3600 G_{sc}}{\pi} \left[1.00011 + 0.034221 \cos \frac{2\pi}{365} t + 0.001280 \sin \frac{2\pi}{365} t \right.$ $\left. + 0.000719 \cos \frac{4\pi}{365} t + 0.00077 \sin \frac{4\pi}{365} t \right]$ $\times \left[\frac{2\pi}{365} t_s \sin L \sin \delta + \cos L \cos \delta \sin t_s \right]$	G_{sc} : Solar constant ($W m^{-2}$) L : Latitude of the study area (degrees) α : Solar altitude (degrees) δ : Sun declination (degrees) t_s : Sunset hour angle (degrees) t : Day of the year
Ratio of diffuse radiation to extraterrestrial radiation on a horizontal plane (τ_b)	$\tau_a = 0.37444 + 0.544175 \exp \left[-\frac{0.31755}{\cos \theta_z} \right]^*$	
Atmospheric transmittance (τ_a)	$\tau_b = 0.271 - 0.2939\tau_a$	
Reflectivity (R_s)	$R_s = A\alpha^B$	A, B : Empirical coefficients functions of cloudiness† θ_z : Zenith angle of the sun
Net long-wave atmospheric radiation (H_{an})	$H_{an} = \varepsilon\sigma(T_{air} + 273)^4(0.684 + 0.0056e_{air})(1 + 0.17C_L^2)$	T_{air} : Air temperature ($^{\circ}C$)
Vapor pressure in the overlying air (e_{air})	$e_{air} = RH \times 6.126 \exp \left[\frac{12.27T_{air}}{237.3 + T_{air}} \right]$	RH : Relative humidity (%) R_L : Reflectivity of the water surface for atmospheric radiation (≈ 0.03)
Surface-emitted longwave radiation (H_b)	$H_b = \varepsilon\sigma(T_{epi} + 273)^4$	σ : Stefan-Boltzmann constant ($4.9 \times 10^{-3} J[m^2 dK^4]^{-1}$) ε : Emissivity of water (≈ 0.97)
Sensible heat fluxes (H_c)	$H_c = c_1 f(U_w)(T_{epi} - T_{air})$	c_1 : Bowen's coefficient (0.47 mm Hg $^{\circ}C^{-1}$)
Wind effects on the transfer	$f(U_w) = 9.2 + 0.52U_w^2$	U_w : Wind velocity ($m s^{-1}$)
Latent heat flux (H_e)	$H_e = f(U_w)(e_s - e_{air})$	
Saturation vapor pressure at the water surface (e_s)	$e_s = 6.126 \exp \left[\frac{17.27T_{epi}}{237.3 + T_{epi}} \right]$	

References: Budyko 1974; Kreith and Kreider 1978; Duffie and Beckman 1980; Brown and Barnwell 1987; Bignami et al. 1995.

* The constants are reported for the standard atmosphere and were corrected for mid-latitude conditions (Duffie and Beckman 1980).

† Brown and Barnwell 1987; see their Table IV-2.

ciated with mass movement of fluids, including eddy diffusion (Edinger et al. 1968).

The heat-budget model was applied from 1969 to 1998 with a time step of 1 d. Initial conditions were based on observed temperature profiles in the lake during the start of the simulation period (22 December 1968). The adjustable parts of the model during the calibration were the formulations that represent the dampening effects of the cloud cover on solar radiation and wind effects on sensible and latent heat transfer. We focused on these components because they have been modeled by a number of different empirical functions that have been applied to water bodies of different size and shape with data averaged over different periods of time (e.g., Brown and Barnwell 1987; Fennessey 2000). In addition, a preliminary sensitivity analysis showed that the modeled processes (i.e., net incoming short-wave radiation and sensible and latent heat transfer) were highly dependent

on the choice of formulation (see also the section ‘‘Sensitivity analysis results with respect to the meteorological variables’’). The selection of the two optimal formulations for the dampening effects of the cloud cover on the solar radiation and wind effects on sensible and latent heat transfer was based on least-squares fitting between simulated and observed epilimnetic and hypolimnetic temperatures.

Results

The mean monthly meteorological data for the study period showed consistent intra-annual patterns (Fig. 1), which accounted for large portions of their overall variability. Partitioning the inter- and intra-annual variation, using hierarchical multivariate analysis of variance, showed that the mean annual cycle explained 95% of the total variability for air temperature, 95% for cloud cover, 94% for rainfall, 88%

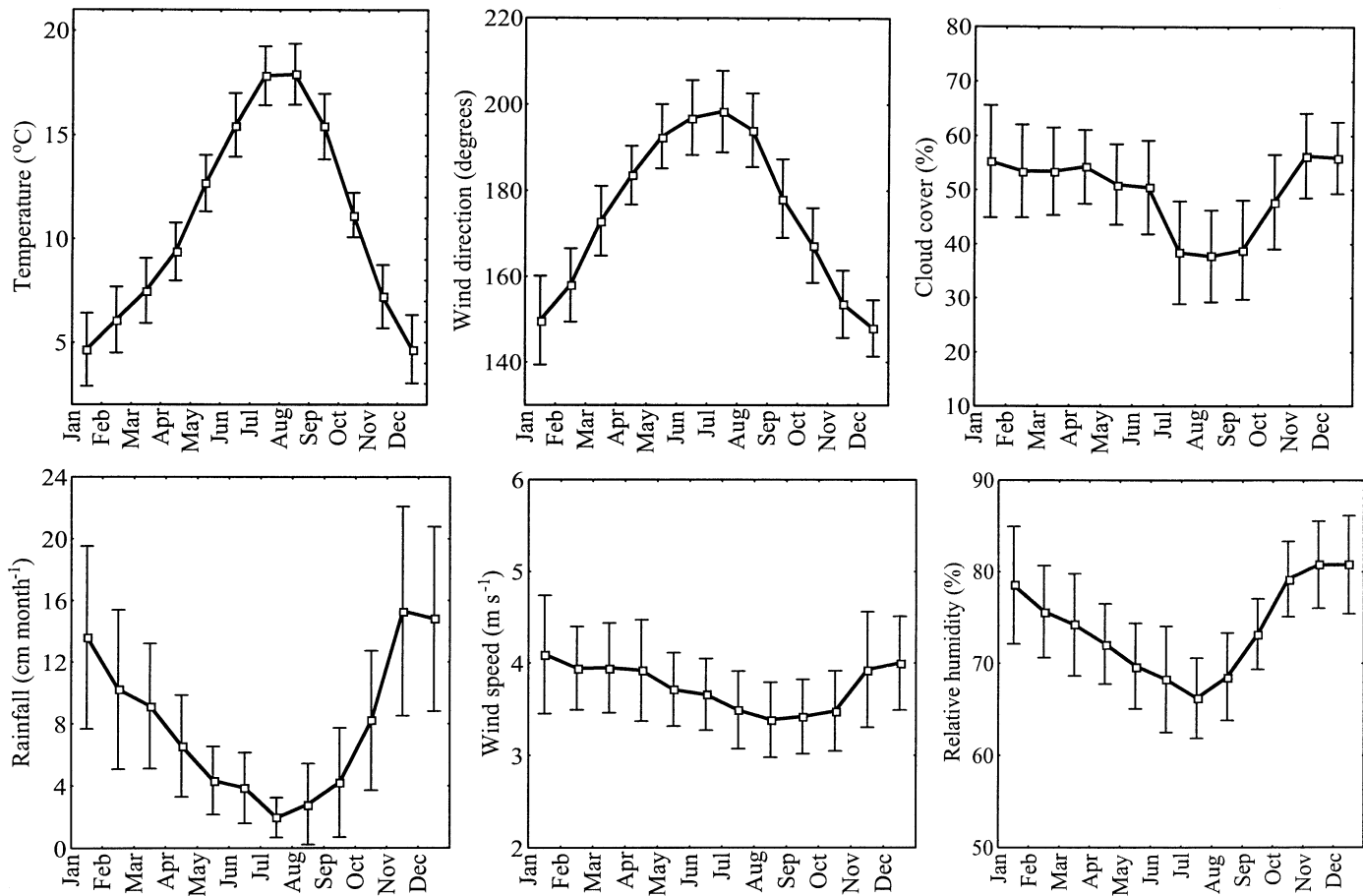


Fig. 1. Annual variability for the air temperature, wind direction, cloud cover, rainfall, wind speed, and relative humidity in the Seattle area, 1964–1999 (data from the SeaTac airport).

for relative humidity, 84% for wind direction, and 67% for wind speed. The long-term annual cycle of volume-weighted Lake Washington temperatures for the 1964–1998 period approximated a sine wave ($r^2 = 0.99$) and was offset from intra-annual variation in solar energy inputs by 50 d (Fig. 2A,B). This annual cycle in lake temperatures explained 93% of the overall variability in mean monthly water temperatures, with the remaining 7% of variation due to inter-annual variation. Figure 2C shows temperature fluctuations at 5 m depth increments over the annual cycle. This figure shows that there was a distinct surface layer ~ 10 m deep, with temperatures $>15^\circ\text{C}$ from June to October. On an annual basis, the volume-weighted upper 10 m of Lake Washington experienced a long-term warming trend with a mean increase of $0.045^\circ\text{C yr}^{-1}$, $r^2 = 0.57$, which corresponds to an increase of 1.5°C over the 35-yr period assessed in the present study. The long-term temperature trend for the deeper parts of the lake was weaker (mean increase: $0.019^\circ\text{C yr}^{-1}$, $r^2 = 0.13$, overall increase: 0.6°C), and the overall volume-weighted mean increase for Lake Washington for the 1964–1998 period was 0.9°C ($0.026^\circ\text{C yr}^{-1}$, $r^2 = 0.30$) (Fig. 3). This warming trend was strongest for the months of April–September and was weakest and nonsignificant for the months November–February for lake volume-weighted temperature. During the time of the year when stratification in

Lake Washington is most intense (i.e., June–September), the long-term warming trend was particularly pronounced for the surface layer (slope $\approx 0.063^\circ\text{C yr}^{-1}$ or 2.2°C for the period assessed). The deeper parts of the lake had a statistically significant warming trend only for the months of March and April (slope $\approx 0.031^\circ\text{C yr}^{-1}$; $r^2 = 0.20$).

The seasonal and trend decomposition for the lake volume-weighted data verified the previously described sinusoidal seasonal pattern with a late-summer maximum (usually in August) and mid- to late-winter minimum (usually in February). According to the rule of N, the first two eigenvalues of the PCA were significantly higher than would have been expected if they were caused by random variability alone. These modes accounted for 79% of the total variance in the monthly time series. Figure 4 presents the first two PCs after varimax rotation. The first mode of variability represents the period of the year when the lake is warming and is warmest (e.g., March–October) and explained 54% of the variability in the overall time series. The corresponding amplitude time series for this mode has a long-term increasing trend, which explains $\sim 32\%$ of the total variance, with the remaining 68% of variability attributable to interannual variability. The second mode was characterized by higher component coefficients during the period when the lake is cooling and is coldest (November–February) and explained 24%

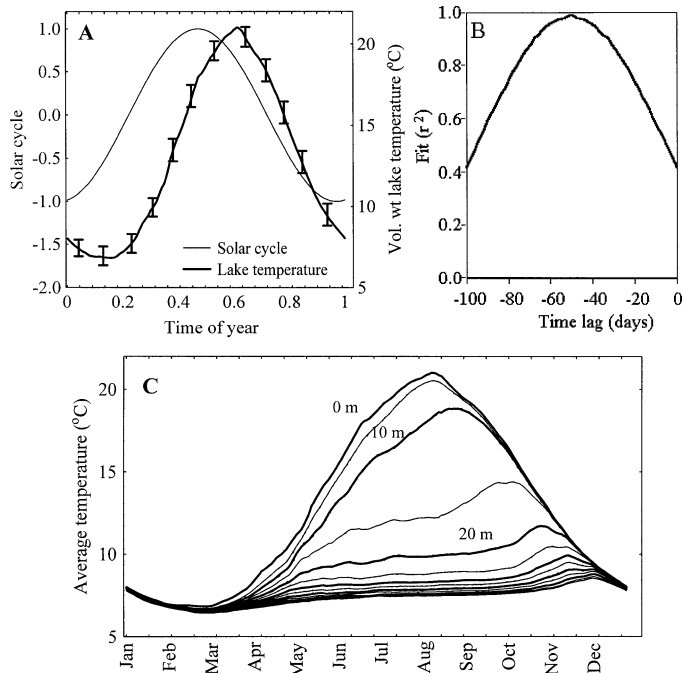


Fig. 2. Comparison of the (A) temperature, (B) solar radiation annual cycle, and (C) mean annual variability of temperature for various depths in Lake Washington.

of the overall variability. The amplitude time-series for this mode was almost exclusively dominated by interannual variability with a minimal long-term trend ($r^2 = 0.02$).

Coefficients of determination (r^2) for regressions between the lake volume-weighted temperature, meteorological variables, and PDO and ENSO indices are presented in Table 2. These relationships are reported for the two modes described by the PCA, to identify potentially causal factors for Lake Washington temperature variability over the annual cycle. Eight- and 4-month averaging windows were used when calculating the environmental variables for modes 1 and 2, respectively. Air temperature ($r^2 = 0.48$), PDO ($r^2 = 0.47$), and MEI ($r^2 = 0.20$) were the best predictors for March–October lake temperature fluctuations (Table 2). Cloud cover ($r^2 = 0.17$), wind speed ($r^2 = 0.12$), and wind direction ($r^2 = 0.19$) had weaker relationships that were, however, statistically significant at the $\alpha = 0.05$ level. The strongest correlations for the second mode (November–February) were with air temperature ($r^2 = 0.43$) and PDO ($r^2 = 0.31$). Statistically significant associations ($\alpha < 0.01$) were also observed for the MEI index ($r^2 = 0.20$) and wind direction ($r^2 = 0.25$). In addition, several meteorological variables, which were not correlated with the first mode, had significant associations with the second: these were solar radiation ($r^2 = 0.15$), relative humidity ($r^2 = 0.15$), and rainfall ($r^2 = 0.14$).

Table 3 presents a comparison of multiple regression models developed to predict Lake Washington water temperatures. The five highest ranked models (according to Mallows's criterion) for both modes of variability included air temperature and PDO as predictors. Solar radiation, relative humidity, and wind speed also appeared to be important for the family of models predicting the second mode. The top-

ranked model for the March–October mode was formed by air temperature and PDO ($r^2 = 0.65$). The respective squared semipartial coefficients, the proportion of variance explained by each predictor relative to the total variance of the dependent variable, were 0.18 and 0.17 (Table 4). In contrast, the best subset of predictors for the November–February mode included PDO ($r^2_{\text{spart}} = 0.28$), air temperature ($r^2_{\text{spart}} = 0.11$), wind speed ($r^2_{\text{spart}} = 0.10$), solar radiation ($r^2_{\text{spart}} = 0.05$), and relative humidity ($r^2_{\text{spart}} = 0.05$) and explained 83% of the overall variability for this mode. Finally, a lack of redundancy (collinearity) between the predictor variables was assessed and verified by computing tolerances (one minus the squared multiple correlation of each variable with all other independent variables in the regression equation), which resulted in values >0.65 for all variables.

Long-term lake heat-budget simulations—This model was used to simulate the thermal dynamics of the lake from 1969 to 1998. As was previously mentioned, during the calibration of the model, two components were adjusted, to obtain the best fit between simulated and observed data. These were cloud cover dampening effects on solar radiation and wind effects on the sensible and latent heat transfer. Eventually, both processes were described using quadratic formulations (Table 1) similar to those used in earlier studies (Budyko 1974; Brown and Barnwell 1987). A comparison between the observed and simulated volume-weighted mean monthly temperatures for the epilimnion ($r^2 = 0.96$, relative error = 12%) and hypolimnion ($r^2 = 0.68$, relative error = 11%) is shown in Fig. 5. The goodness-of-fit statistics indicate that the model accurately reproduced the thermal dynamics of the lake, whereas the lower coefficient of determination value for the hypolimnion is largely a statistical artifact, because there is much less variability in the hypolimnetic monthly time series. A quantitative assessment of the contribution of the various heat sources and sinks over the simulation period is presented in Fig. 6, where the squares correspond to the net annual values of the five heat fluxes in the model. According to the model's estimates, the heat contribution from net short-wave solar and long-wave atmospheric radiation was, on average, 132 ± 5 and 306 ± 6 $\text{W m}^{-2} \text{ yr}^{-1}$, whereas the lake lost 363 ± 4 , 74 ± 6 , and 6 ± 2 $\text{W m}^{-2} \text{ yr}^{-1}$ through surface-emitted long-wave radiation and latent and sensible heat fluxes, respectively. In general, interannual variability dominated the patterns, especially for the net short-wave radiation and latent and sensible heat fluxes. Significant long-term linear trends were primarily observed for surface-emitted long-wave radiation ($r^2 = 0.53$) and for atmospheric long-wave radiation ($r^2 = 0.24$).

Sensitivity analyses with respect to meteorological variables—Precise uncertainty estimates for models like the one developed for the present study are not feasible, because they include empirical equations or coefficients whose associated errors are difficult or impossible to estimate and whose parameter uncertainty is, in most cases, unknown. However, the structure of the model and the nature of the results can be explored through an analyses of model sensitivity to input variables, which in the present case were air temperature, relative humidity, cloudiness, and wind speed. We analyzed

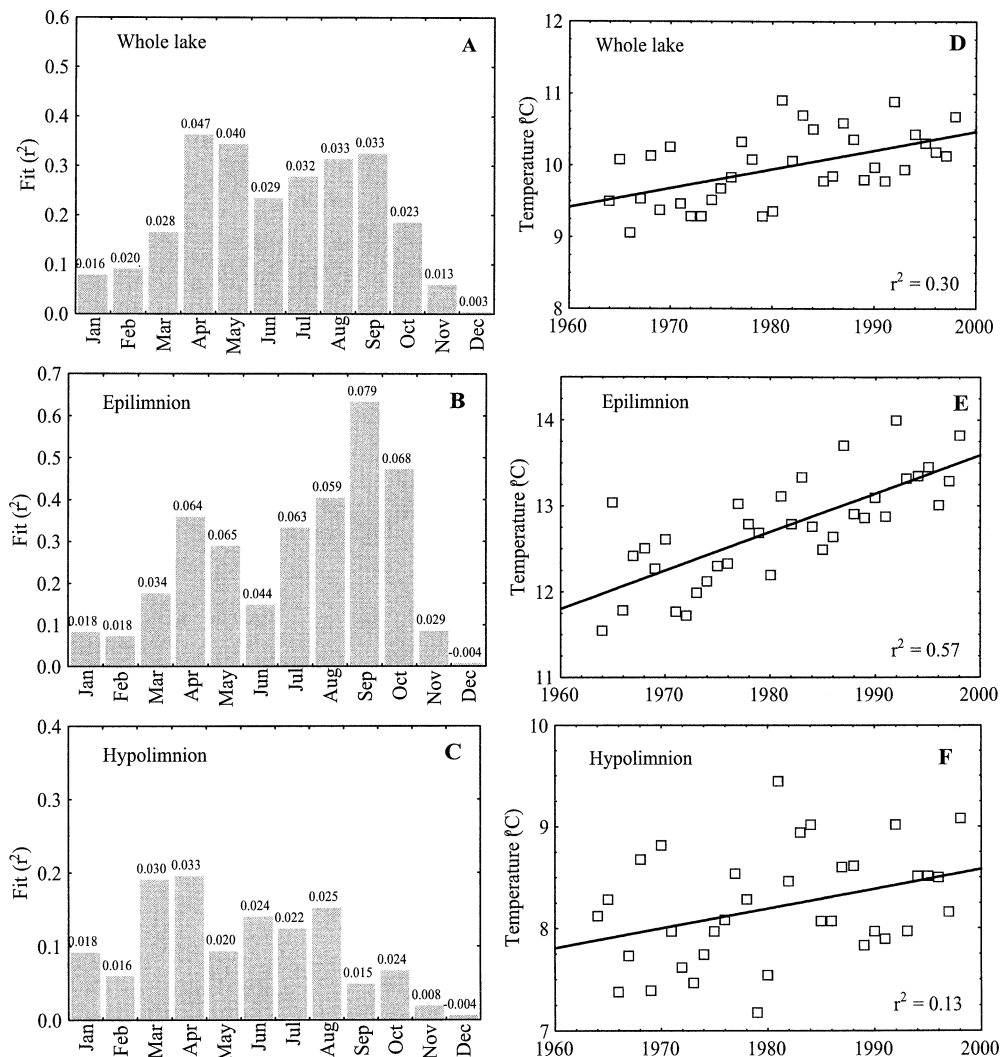


Fig. 3. (A–C) Individual month and (D–F) annual trends in Lake Washington, 1964–1999. The Y-axis of the individual month panels indicate the coefficient of determination (r^2) of the linear trends, whereas the numbers over the bars indicate the respective slopes ($^{\circ}\text{C yr}^{-1}$).

the influence of the four meteorological input variables on the two state variables (epilimnion and hypolimnion temperature) and the five fluxes of the model by creating 100 randomly generated data sets for each of the input variables (Monte Carlo simulations). This was done by taking the original input variable data set and randomly increasing or decreasing each value by a coefficient obtained from a normal distribution with a mean value 1 and standard deviation 0.1 ($0 \pm 10\%$ change of the actual value of the meteorological variable). (Note that the coefficients of variation for the interannual variability of the four meteorological input variables were between 5% and 9%). Table 5 presents this quantification of model output dependence (total averages over the simulation period) on input meteorological variables (induced perturbations), with general linear models used to examine these relationships. Air temperature accounted for a substantial proportion of the variability for the two state variables (54% and 43% for epilimnion and hypolimnion temperatures, respectively) as well as atmospheric long-wave

(56%) and surface-emitted long-wave radiation (55%). The two matter-linked heat-transfer mechanisms (sensible and latent) appeared to be almost equally sensitive to relative humidity and cloudiness variation, whereas net short-wave radiation was exclusively dependent on cloudiness effects (99%). Moreover, the two fluxes that had linear trends over the 30-yr simulation period were also sensitive to cloud cover (21% and 16% for the atmospheric long-wave and the surface-emitted long-wave radiation). Additionally, 19% of the surface-emitted long-wave radiation variation could be explained by relative humidity. These statistical analyses also included the contribution of the higher order, interactive effects for the input meteorological variables, which were, however, not found to be significant for the model behavior.

Discussion

We analyzed a 35-yr record of Lake Washington temperature data to test for long-term trends in this lake's thermal

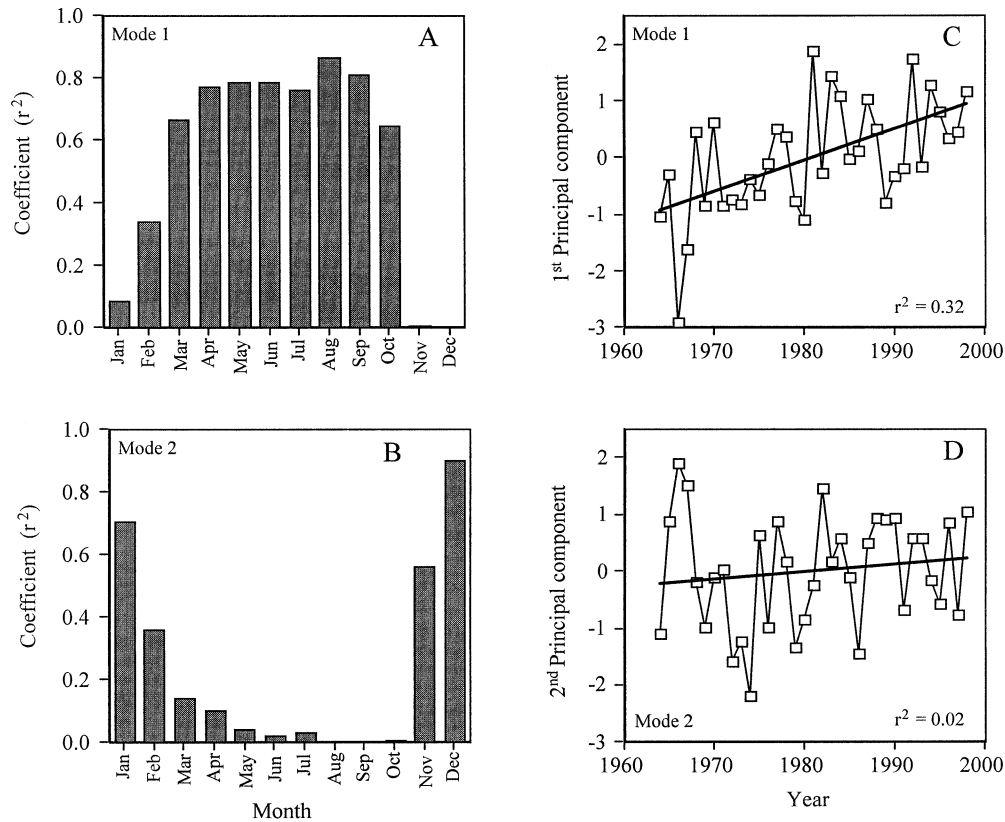


Fig. 4. (A, B) Squared component coefficients and (C, D) amplitudes for the two PCs of temperature for data weighted over the total lake volume.

properties and to identify the basic forces driving interannual variability. This analysis found volume-weighted Lake Washington temperatures have increased on average by $0.026^{\circ}\text{C yr}^{-1}$ (or 0.9°C during the 35-yr period assessed). This warming trend was most pronounced for the epilimnion

Table 2. Coefficients of determination (r^2) between water temperature (lake volume weighted data) and the meteorological variables, the PDO and the MEI indices. An 8-month window was used when calculating the environmental variables for mode 1 and a 4-month window was used when calculating variables for mode 2. The parentheses indicate the lag (months) between the variables that results in the highest coefficient of determination.

Variable	(March–October)	(November–February)
1st mode	0.96*	0.09
2nd mode	0.04	0.89*
Air temperature	0.48* (-2)	0.43* (-1)
Relative humidity	0.04 (-3)	0.15† (-1)
Wind speed	0.12† (0)	0.12‡ (-1)
Wind direction	0.19† (-1)	0.25* (0)
Cloud cover	0.17‡ (-4)	0.10‡ (-2)
Solar radiation	0.05 (-1)	0.15† (-2)
Rainfall	0.05‡ (-3)	0.14‡ (-2)
PDO	0.47* (-4)	0.31† (0)
MEI	0.20* (-2)	0.20† (-6)

* Significant at the 1% level.

† Significant at the 5% level.

‡ Negative correlation.

during the stratified period, which has warmed 2.2°C during the study period. These results support the findings of other studies, which have reported evidence of warming trends or significant changes in the thermal structure of North American lakes (e.g., Schindler et al. 1996; King et al. 1997; McCormick and Fahnenstiel 1999). The stratification trends noted in Lake Washington (i.e., more intense epilimnetic than whole lake warming) are similar to what King et al. (1997) reported for regions of Lake Huron, which those authors attributed to changed climatic conditions. McCormick and Fahnenstiel (1999) also observed warming trends in near-shore sites of the Great Lakes and an increase in the duration of the stratified period, which was mostly due to an earlier transition to springlike conditions. Lake Washington’s hypolimnion has also warmed by $\sim 0.6^{\circ}\text{C}$. Peeters et al. (2002) described similar hypolimnetic warming for Lake Zurich under increased air temperature scenarios, which they attributed to the large depth of Lake Zurich and hypolimnetic heat carryover from year to year. This climate-induced hypolimnetic warming is a characteristic of large, warm monomictic lakes, which are not reset to 4°C each winter as are dimictic lakes.

We split the annual temperature time series into two independent seasonal “modes” of variability, which together accounted for 79% of the total observed variance in Lake Washington’s thermal conditions. The first mode represented the period of the year when the lake is warming and/or is stratified (March–October), and this mode exhibited a de-

Table 3. Comparison of regression models developed for predicting water temperature (lake-volume weighted data) in Lake Washington. Rank is assigned in order of increasing Mallows' criterion, which was used to select the best subset of predictor variables. The parentheses indicate the lag (months) between the variables that resulted in the highest coefficient of determination (see Table 2).

Mallows' Number of		Predictors					
Rank	criterion	X1	X2	X3	X4	X5	X6
1st mode (March–October)							
1	-2.09	Air temperature (-2)	PDO (-4)				
2	-2.00	Air temperature (-2)	PDO (-4)	Cloud cover (-4)			
3	-1.89	Air temperature (-2)	PDO (-4)	Relative humidity (-3)			
4	-1.09	Air temperature (-2)	PDO (-4)	Cloud cover (-4)	Relative humidity (-3)		
5	-0.82	Air temperature (-2)	PDO (-4)	Wind speed (0)			
2nd mode (November–February)							
1	0.36	Air temperature (-1)	PDO (0)	Relative humidity (-1)	Solar radiation (-2)	Wind speed (-1)	
2	2.08	Air temperature (-1)	PDO (0)	Relative humidity (-1)	Cloud cover (-2)*	Wind speed (-1)	
3	2.29	Air temperature (-1)	PDO (0)	Relative humidity (-1)	Solar radiation (-2)	Wind speed (-1)	ENSO (-6)*
4	2.31	Air temperature (-1)	PDO (0)	Relative humidity (-1)	Solar radiation (-2)	Wind speed (-1)	ENSO (-5)*
5	2.33	Air temperature (-1)	PDO (0)	Relative humidity (-1)	Solar radiation (-2)	Wind speed (-1)	Cloud cover (-2)

* Negative sign of the regression model parameter.

cadal-scale trend as well as year-to-year variability around this trend. Air temperature appeared to be an important driving force for Lake Washington temperatures during this period, which is not surprising, given that air and water temperature (especially for the epilimnion) are often highly correlated on both short and long timescales (e.g., Shuter et al. 1983; Livingstone and Dokulil 2001). During the same period, the PDO index was an equally good predictor for water temperature. To our knowledge, these results are the first to demonstrate strong PDO effects on the thermal properties of a lacustrine ecosystem. In contrast, there are numerous published examples of PDO effects on marine systems, including primary and secondary production (e.g., Roemmich and McGowan 1995; Brodeur et al. 1996), fisheries production (e.g., Hare et al. 1999), and even marine mammals (Francis et al. 1998). The best correlation between Lake Washington temperature and the PDO resulted from a backward shift (-4 months) of the 8-month window toward the winter months, when year-to-year PDO fluctuations are most pronounced (Zhang et al. 1997). The North American climate anomalies associated with PDO are broadly similar to those associated with ENSO anomalies (i.e., El Niño and La Niña), although they are generally not as extreme and are at a different temporal scale (Mantua and Hare 2002). Willmott and Matsuura (2000) reported correlations between the November–April mean PDO index and the respective mean precipitation and temperatures, which suggests that the warm phase of the PDO coincides with anomalously dry weather and warm temperatures in northwestern North America with the opposite pattern seen during the cool phase. Analogous results were reported by Hare and Mantua (2000), who showed that winter air temperatures for six northwest North American coastal sites were correlated with the PDO. In our data set, we found a coefficient of determination of 0.21 between air temperature and PDO, whereas the two variables together explained ~65% of the total variability observed for March–October lake temperatures. It is also notable that the PDO signature on water temperatures explained 17% of the variability and that air temperature explained an additional 18% (see Table 4, r^2_{spart} values). The ENSO signal was clearly weaker during this period, which should be attributed to the fact that our analysis was based on overall lake volume-weighted data. When we separately correlated the epilimnion (0–10 m) and hypolimnion (10 m–bottom) temperatures with the PDO and ENSO indices, we found that the ENSO correlation with surface layer temperatures ($r^2 = 0.41$) was almost as strong as the PDO correlation ($r^2 = 0.46$). However, the ENSO correlation with water temperature was much weaker in the hypolimnion ($r^2 = 0.09$), whereas the PDO signature was significant ($r^2 = 0.35$) and characterized by a 5-month backward shift of the 8-month window. This suggests that hypolimnetic warming in large monomictic lakes is more responsive to longer time-scale climatic phenomena like the PDO.

The second mode identified in our PCA represents the period during the year when the lake is cooling and becomes isothermal (November–February) and is dominated by interannual variability without a long-term trend. Air temperature and PDO (with no lag) were again the best individual predictor variables for lake temperatures during this mode.

Table 4. Final regression models developed for predicting water temperature (lake-volume weighted data) in Lake Washington. Symbols β , β_o , r^2_{part} , and s denote the coefficient of each predictor, the intercept, the squared semi-partial coefficient, and the SE of the estimate for the models, ranked first according to the Mallows's criterion.

Variable	β	β_o	r^2_{part}	s	$F_{(DF_{\text{pred}}/DF_{\text{resid}})}$	P	r^2
1st mode (March–October)							
Air temperature	0.41	5.79	0.18	0.35	29.81	0.00	0.65
PDO	0.29		0.17				
2nd mode (November–February)							
Air temperature	0.23	0.74	0.11	0.22	19.99	0.00	0.83
PDO	0.32		0.28				
Relative humidity	0.03		0.05				
Solar radiation	0.03		0.05				
Wind speed	0.54		0.10				

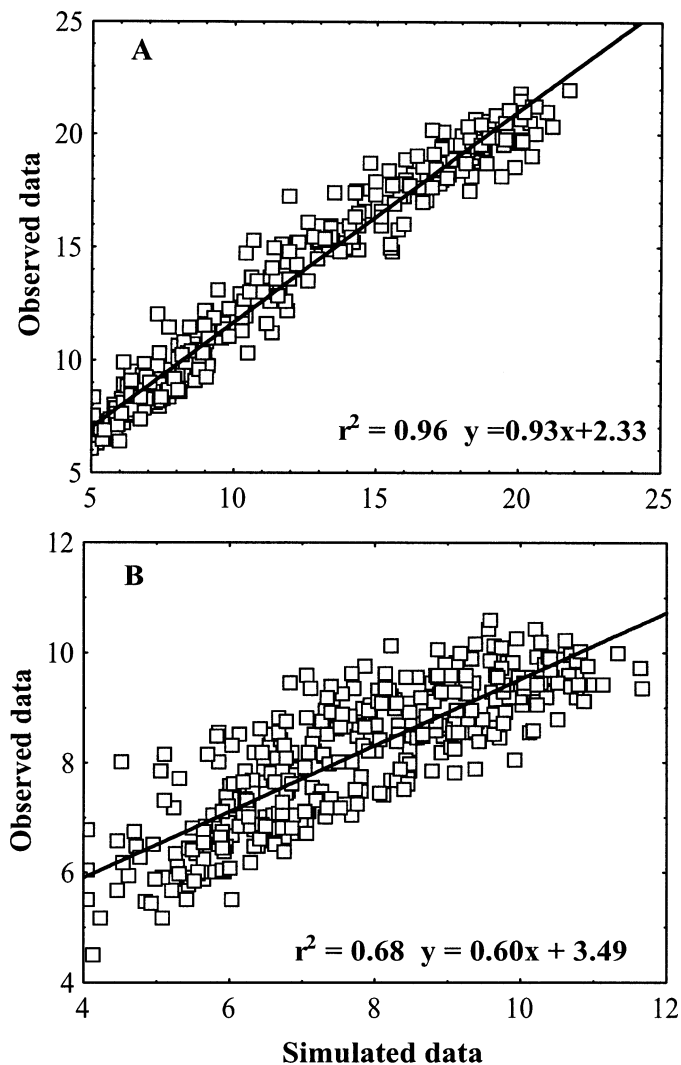


Fig. 5. Heat-budget model for Lake Washington. Observed vs. predicted monthly (A) epilimnion and (B) hypolimnion water temperatures.

The best multiple regression model showed $r^2 = 0.83$, with the PDO explaining 28% of the overall variability. Solar radiation, relative humidity, and wind speed also seemed to play important roles during this period, and their combined net contribution toward an explanation of lake thermal dynamics was $\sim 20\%$. These three meteorological variables are related to heat-exchange processes that help determine the heat balance of the lakes (Budyko 1974). Therefore, we tried to relate temperature values for the second mode to the November–February averages for the five mechanisms (net short-wave solar radiation, net long-wave atmospheric radiation, surface-emitted longwave radiation, and sensible and latent heat fluxes) as computed by the heat-budget model. The highest correlations were found for sensible ($r^2 = 0.30$) and latent ($r^2 = 0.21$) heat fluxes, which were closely coupled with wind speed. Latent heat is also related to relative humidity. Moreover, these meteorological variables had high interannual variability during these months (see the November–February error bars in Fig. 1), and this is probably one reason why the air temperature and PDO signals are weakened and the second mode, in contrast with the first one, does not show a long-term trend.

Our study also includes the period when the wastewater discharges to the lake were progressively decreased to zero (1964–1968), the subsequent transient phase (1969–1974), and the establishment of a new equilibrium state from 1975 to the present (Edmondson and Lehman 1981). Changes in water clarity due to the diversion of wastewater and resurgence of *Daphnia* could have induced changes in the thermal structure of Lake Washington (Mazumder and Taylor 1994). Therefore, we regressed the residuals of the multiple regression models developed for the two modes of variability against the corresponding Secchi depth observations. The resulting coefficients of determination were 0.04 and 0.01 for the first and second modes of variability, respectively, which suggests that water clarity had little effect on Lake Washington's thermal properties. However, these results cannot be directly compared with those of Mazumder and Taylor (1994), because our analysis looked at overall volume-weighted lake temperatures, whereas Mazumder and Taylor noted trends between water clarity and epilimnion depth. In all likelihood, water clarity will manifest its greatest effects on the surface layer of lakes (e.g., epilimnion depth and temperature) and will have little or no effect on deeper strata.

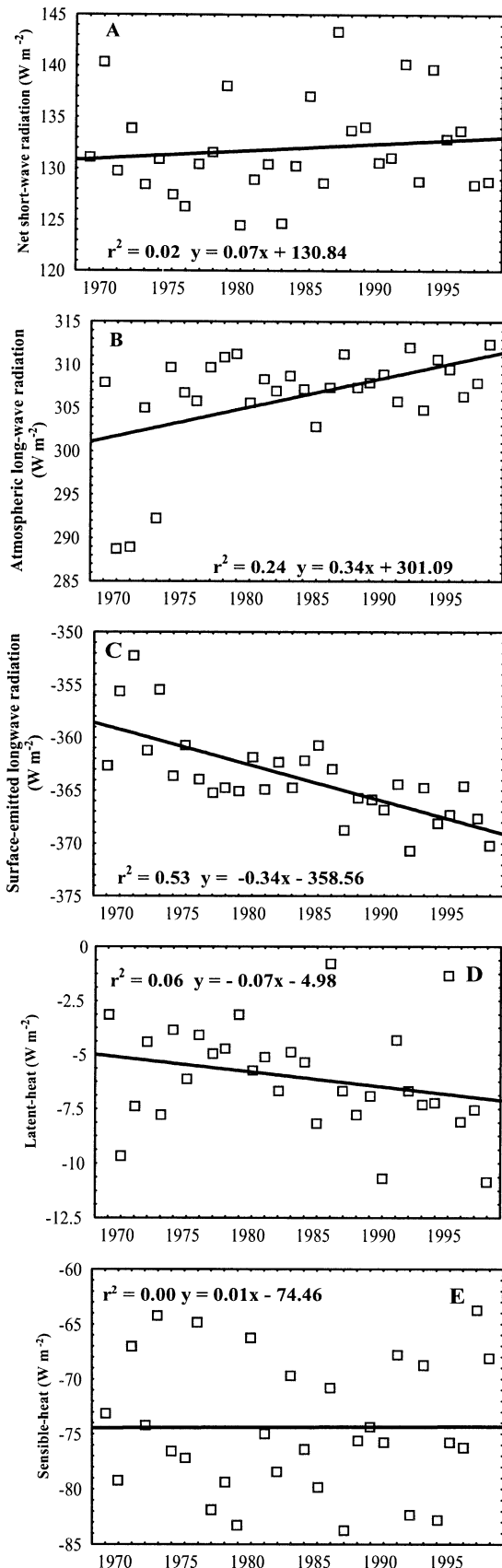


Fig. 6. Annual fluxes of heat ($W m^{-2}$), as computed from the heat-budget model for Lake Washington.

Table 5. Regression models ($n = 100$) based on the Monte Carlo analysis of the heat budget model. The symbol r_{spart}^2 corresponds to the squared semi-partial coefficient.

Dependent and independent variables	r_{spart}^2
Epilimnion temperature	
Wind speed	0.05
Air temperature	0.54
Relative humidity	0.20
Cloudiness	0.15
Hypolimnion temperature	
Wind speed	0.08
Air temperature	0.43
Relative humidity	0.28
Cloudiness	0.15
Sensible heat fluxes	
Wind speed	0.04
Air temperature	0.04
Relative humidity	0.51
Cloudiness	0.38
Net short-wave radiation	
Cloudiness	0.99
Atmospheric long-wave radiation	
Air temperature	0.56
Relative humidity	0.09
Cloudiness	0.21
Surface-emitted long-wave radiation	
Wind speed	0.04
Air temperature	0.55
Relative humidity	0.19
Cloudiness	0.16
Latent heat fluxes	
Wind speed	0.08
Air temperature	0.08
Relative humidity	0.49
Cloudiness	0.53

The contribution of all the main and higher-order interactive effects of the input meteorological variables was tested, but this table only shows the significant factors.

Therefore, further study of water clarity effects on surface temperatures and epilimnion depth in Lake Washington would be warranted.

Heat-budget model—The basic purpose for developing the model was to quantitatively assess the various heat sources and sinks for the lake. The estimates for the absolute and relative magnitudes of the five heat-exchange processes were consistent with previously reported values (Budyko 1974; Kreith and Kreider 1978; Duffie and Beckman 1980; Brown and Barnwell 1987; Bignami et al. 1995). Moreover, the model output suggested that year-to-year variability dominated the patterns for the heat-exchange processes, especially for net short-wave radiation and sensible and latent heat fluxes. Significant long-term trends were only found for atmospheric long-wave and surface-emitted long-wave radiation. Although the latter process is just the increase in long-wave radiation emission due to water surface warming, the former process is possibly linked to climatic change. The

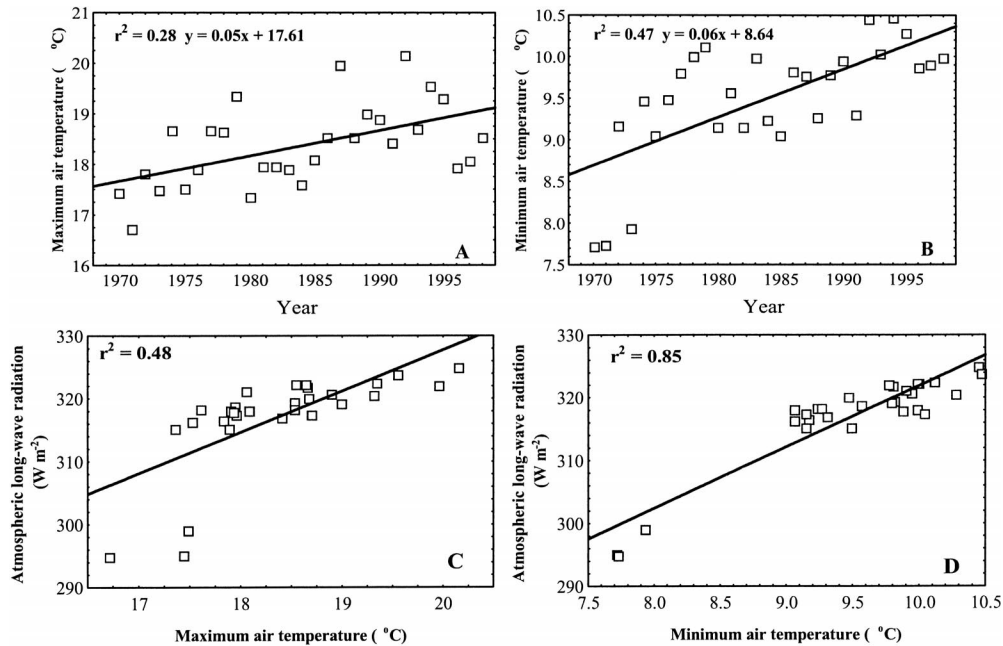


Fig. 7. Trends of the average daily maximum and minimum values of temperature ($^{\circ}\text{C}$) over the first mode of variability (March–October) and the respective bivariate plots with the atmospheric long-wave radiation (W m^{-2}). The meteorological data are from the SeaTac Airport weather station.

heat-budget model sensitivity analysis showed that the atmospheric long-wave radiation component is correlated with air temperature (56%), cloud cover (21%), and relative humidity (9%). Apparently, these three meteorological variables have, during the past 35 yr, promoted increasing amounts of incoming long-wave radiation, possibly through the absorption and counterradiation of the long-wave fluxes emitted by the Earth's surface. It should also be pointed out that the linear trend in atmospheric long-wave radiation was most evident for the first mode (March–October) with slope = $0.525 \text{ W m}^{-2} \text{ yr}^{-1}$ and $r^2 = 0.35$.

We attempted to validate these results by relating them to other climate changes in the region. Several studies have shown that the rise in the global mean surface temperature has resulted, at least in part, from the daily minimum temperature increasing at a faster rate than the daily maximum, resulting in a decrease in the diurnal temperature range (Easterling et al. 1997). These trends can also provide plausible explanations for the mechanisms that drive changes in the thermal structure of aquatic ecosystems. For example, Livingstone (2003) found that epilimnetic temperature increases in Lake Zurich were closely related to increased daily minimum air temperatures, whereas a clear decreasing rate of nighttime heat loss was associated with the absorption of atmospheric long-wave radiation, evaporative heat exchange, and the convective exchange of sensible heat. Therefore, we calculated average daily maximum and minimum air temperatures over the first mode of variability (March–October)—the period when we found significant decadal-scale temperature trends. The slopes of the maximum and minimum air temperatures were 0.05 ($r^2 = 0.28$) and $0.06^{\circ}\text{C yr}^{-1}$ ($r^2 = 0.47$); moreover, they were highly correlated with the atmospheric long-wave radiation (March–October average),

with the respective r^2 values being 0.48 and 0.85 (Fig. 7). However, caution should be exercised when interpreting these results for two basic reasons. (1) The slight difference in the daily minimum and maximum air temperature increases computed for Lake Washington are in contrast to the fairly clear situation described in Lake Zurich (*see* figure 5 of Livingstone 2003), where a long-term increase in epilimnetic temperature was compared with a similar long-term increase in daily minimum air temperature and contrasted with a long-term decrease in daily maximum air temperature. (2) Our data include three outliers (years 1970, 1971, and 1973) that seem to influence the results. Removing these outliers and recalculating the regressions, we found similar increases for maximum ($0.035^{\circ}\text{C yr}^{-1}$, $r^2 = 0.14$) and minimum ($0.030^{\circ}\text{C yr}^{-1}$, $r^2 = 0.29$) air temperatures, whereas the respective r^2 values for atmospheric long-wave radiation were 0.64 and 0.59. (Note that the significant long-term trend in the atmospheric long-wave radiation [March–October average] still exists even after the exclusion of the outliers; slope = $0.13 \text{ W m}^{-2} \text{ yr}^{-1}$; $r^2 = 0.13$). In addition, the maximum air temperatures were significantly negatively correlated with the sensible heat losses ($r^2 = 0.30$). This relationship was not affected by the presence of the outliers ($r^2 = 0.31$).

We also considered the fact that Lake Washington is located within the Seattle metropolitan area, which has had a steadily increasing population during the study period. Therefore, some of the observed temperature trends could be due to an increasing urban heat island effect. Hence, we estimated heat island trends over the study period. We did this by comparing air temperature differences between one urban (SeaTac) and two rural (Snoqualmie Falls and Startup) meteorological stations for the 1964–1998 period. Neither the average ($0.005^{\circ}\text{C yr}^{-1}$; $r^2 = 0.016$), maximum (0.011°C

yr⁻¹; $r^2 = 0.058$), nor minimum ($-0.007^\circ\text{C yr}^{-1}$; $r^2 = 0.026$) air temperature differences showed significant increasing trends, which indicates that any increase in the Seattle metropolitan area heat island effect during the period considered in this study was minimal.

Biological response—Compelling evidence for structural shifts in Lake Washington's plankton and fish populations associated with climatic perturbations have not yet been reported, because, so far, most studies of Lake Washington have been focused on this system's recovery from severe eutrophication (Edmondson 1997). Although the biological responses to climatic forcing are considered to be more variable owing to the complex nature of factors that determine ecological interactions in lakes (Carpenter et al. 1992; De Stasio et al. 1996), long-term trends or, at least, year-to-year fluctuations are possible. Indeed, recent studies have reported associations of large-scale meteorological phenomena with changes in plankton dynamics (Arhonditsis et al. unpubl. data; Winder et al. unpubl. data), such as the timing of the spring bloom and temporal shifts in the clear water phase in Lake Washington. Furthermore, sockeye salmon (*Oncorhynchus nerka*) juveniles obtain some of the highest recorded growth rates throughout their range in Lake Washington (Ballantyne et al. 2003), and sockeye salmon responses to temperature changes are both ecologically and economically important. Several studies have linked the Pacific Decadal Variability with 20th-century Pacific salmon catches (e.g., Beamish et al. 1999). Quinn et al (1997) related the timing of adult sockeye spawning migrations to changing flow and temperature regimes over the past several decades and showed that, despite favorable growing conditions in the ocean during the summer, some sockeye populations at the southern end of their range return to freshwater during late spring or early summer and then stay in lakes near their natal streams for several months before spawning in the fall. Hodgson and Quinn (2002) hypothesized that these migration timing patterns are the "best of a bad situation" and that good ocean growing conditions were passed up so that this fish could avoid stressful high summer temperatures and still be able to access suitable spawning areas in the fall. Using a critical temperature of 19°C for sockeye salmon, these authors showed that sockeye salmon populations migrate before or after the warm period (sometimes several months before spawning in the former case) in freshwater systems that exceed this critical value. Lake Washington's sockeye salmon population is consistent with these patterns, and an early migration (33 d difference between the migration date and the date of peak average temperature; see Table 2 of Hodgson and Quinn 2002) before spawning helps to avoid the higher surface temperatures (20–22°C) that will be encountered during summer stratification. However, given the warming trends noted for Lake Washington in this study, longer spawning migration delays are likely to be triggered, with adverse repercussions for fish reproductive potential, especially egg size and fecundity (Hodgson and Quinn 2002). In addition, the warming trends in Lake Washington were associated with an observed proliferation of warm-water fishes (e.g., small-mouth bass) and the increased predation rates of warm-water piscivores, especially during

springtime, when salmon smolts migrate out through the Lake Union/ship canal system (Stock et al. unpubl. data). If the increasing water temperature trends noted for Lake Washington are also indicative of trends in other Pacific northwest lake/salmon systems—which are already on the upper level of thermal tolerances during critical life history stages such as Columbia River Basin (Melack et al. 1997), Upper Klamath Lake and Lake Shasta (National Research Council 2002; Nickel et al. unpubl.)—then these results could suggest dire consequences for some Pacific northwest salmonid populations in the future.

Statistical analyses of long-term temperature records from Lake Washington, Washington, showed a warming trend with a mean increase of 0.026°C yr⁻¹ for overall lake temperatures that is most strongly associated with air temperatures and the PDO. This warming trend was much stronger for the epilimnion during the summer stratified period (0.063°C yr⁻¹). Although positively correlated, the two signals (air temperature and PDO) have distinct signatures that vary in relative importance over the annual cycle for this lake. We were able to associate the air temperature trends with other local climatic patterns (maximum and minimum temperature increasing rates) and mechanisms of radiative heat exchange (e.g., long-wave radiation and sensible heat losses), but urban heat island effects were found to be negligible. The most important next step is to determine how chemical and biological components of Lake Washington will respond to these changes in the thermal properties.

References

- ADRIAN, R., R. DENEKE, U. MISCHKE, R. STELLMACHER, AND P. LEDERER. 1995. Long-term study of the Heiligensee (1975–1992)—evidence for effects of climatic-change on the dynamics of eutrophied lake ecosystems. *Arch Hydrobiol.* **133**: 315–337.
- AEBISCHER, N. J., J. C., COULSON, AND J. M. COLEBROOK. 1990. Parallel long-term trends across 4 marine trophic levels and weather. *Nature* **347**: 753–755.
- BALLANTYNE, A. P., M. T. BRETT, AND D. E. SCHINDLER. 2003. The importance of dietary phosphorus and highly unsaturated fatty acids for sockeye (*Oncorhynchus nerka*) growth in Lake Washington—a bioenergetics approach. *Can. J. Fish. Aquat. Sci.* **60**: 12–22.
- BEAMISH, R. J., D. J. NOAKES, G. A. MCFARLANE, L. KLYASHTORIN, V. V. IVANOV, AND V. KURASHOV. 1999. The regime concept and natural trends in the production of Pacific salmon. *Can. J. Fish. Aquat. Sci.* **56**: 516–526.
- BIGNAMI, F., S. MARULLO, R. SANTOLERI, AND M. E. SCHIANO. 1995. Long-wave radiation budget in the Mediterranean Sea. *J. Geophys. Res.* **100**: 2501–2514.
- BRODEUR, R. D., B. W. FROST, S. R. HARE, R. C. FRANCIS, AND W. J. INGRAHAM JR. 1996. Interannual variations in zooplankton biomass in the Gulf of Alaska, and covariation with California current zooplankton biomass. *Cal. Coop. Ocean. Fish.* **37**: 80–99.
- BROWN, L. C., AND T. O. BARNWELL JR. 1987. The enhanced stream water quality models QUAL2E and QUAL2E-UNCAS: Documentation and users manual. Report EPA/600/3-87/007. U.S. Environmental Protection Agency.
- BUDYKO, M. I. 1974. *Climate and life*. Academic Press.
- CARPENTER, S. R., S. G. FISHER, N. B. GRIMM, AND J. F. KITCHELL.

1992. Global change and freshwater ecosystems. *Annu. Rev. Ecol. Syst.* **23**: 119–139.
- DESTASIO, B. T., D. K. HILL, J. M. KLEINHANS, N. P. NIBBELINK, AND J. J. MAGNUSON. 1996. Potential effects of global climate change on small north-temperate lakes: Physics, fish, and plankton. *Limnol. Oceanogr.* **41**: 1136–1149.
- DUFFIE, J. A., AND W. A. BECKMAN. 1980. Solar engineering of thermal processes. John and Wiley & Sons.
- EASTERLING, D. R., AND OTHERS. 1997. Maximum and minimum temperature trends for the globe. *Science* **277**: 364–367.
- EDINGER, J. E., D. W. DUTTWEILER, AND J. C. GEYER. 1968. The response of water temperatures to meteorological conditions. *Water Resour. Res.* **4**: 1137–1143.
- EDMONDSON, W. T. 1997. Aphanizomenon in Lake Washington. *Arch. Hydrobiol. Suppl.* **107**: 409–446.
- , AND J. T. LEHMAN. 1981. The effect of changes in the nutrient income on the condition of Lake Washington. *Limnol. Oceanogr.* **26**: 1–29.
- FENNESSEY, N. M. 2000. Estimating average monthly lake evaporation in the northeast United States. *J. Am. Water Resour. Assoc.* **36**: 759–769.
- FRANCIS, R. C., S. R. HARE, A. B. HOLLOWED, AND W. S. WOOSTER. 1998. Effects of interdecadal climate variability on the oceanic ecosystems of the NE Pacific. *Fish Oceanogr.* **7**: 1–21.
- GEORGE, D. G., J. F. TALLING, AND E. RIGG. 2000. Factors influencing the temporal coherence of five lakes in the English Lake District. *Freshw. Biol.* **43**: 449–461.
- , AND A. H. TAYLOR. 1995. UK lake plankton and the Gulf Stream. *Nature* **378**: 139.
- GERTEN, D., AND R. ADRIAN. 2000. Climate-driven changes in spring plankton dynamics and the sensitivity of shallow polymictic lakes to the North Atlantic Oscillation. *Limnol. Oceanogr.* **45**: 1058–1066.
- , AND ———. 2001. Differences in the persistency of North Atlantic Oscillation signals among lakes. *Limnol. Oceanogr.* **46**: 448–455.
- GOLDMAN, C. R., A. D. JASSBY, AND T. M. POWELL. 1989. Interannual fluctuations in primary production: Meteorological forcing as two subalpine lakes. *Limnol. Oceanogr.* **34**: 310–323.
- HARE, S. R., AND N. J. MANTUA. 2000. Empirical evidence for North Pacific regime shifts in 1977 and 1989. *Prog. Oceanogr.* **47**: 103–145.
- , AND R. C. FRANCIS. 1999. Inverse production regimes: Alaskan and West Coast Salmon. *Fisheries* **24**: 6–14.
- HODGSON, S., AND T. P. QUINN. 2002. The timing of adult sockeye salmon migration into fresh water: Adaptations by populations to prevailing thermal regimes. *Can. J. Zool.* **80**: 542–555.
- HOSTETLER, S. W., AND E. E. SMALL. 1999. Response of North American freshwater lakes to simulated future climates. *J. Am. Water Resour. Assoc.* **35**: 1625–1637.
- IDSO, S. B., AND R. G. GILBERT. 1974. On the universality of the Poole and Atkins Secchi disk-light extinction equation. *J. Appl. Ecol.* **11**: 399–401.
- JASSBY, A. D. 1999. Uncovering mechanisms of interannual variability from short ecological time series, p. 285–306. *In* K. M. Scow, G. E. Fogg, D. E. Hinton, and M. L. Johnson [eds.], *Integrated assessment of ecosystem health*. CRC Press.
- , J. E. CLOERN, AND B. E. COLE. 2002. Annual primary production: Patterns and mechanisms of change in a nutrient-rich tidal ecosystem. *Limnol. Oceanogr.* **47**: 698–712.
- , T. M. POWELL, AND C. R. GOLDMAN. 1990. Interannual fluctuations in primary production: Direct physical effects and the trophic cascade at Castle Lake, California. *Limnol. Oceanogr.* **35**: 1021–1038.
- KENDALL, M., AND J. K. ORD. 1990. *Time series*. 3rd ed. Griffin.
- KING COUNTY. 2002. Water quality monitoring of northern Lake Washington streams. King County Department of Natural Resources and Parks.
- KING, J. R., B. J. SHUTER, AND A. P. ZIMMERMAN. 1997. The response of the thermal stratification of South Bay (Lake Huron) to climatic variability. *Can. J. Fish. Aquat. Sci.* **54**: 1873–1882.
- KREITH, F., AND J. F. KREIDER. 1978. *Principles of solar engineering*. Hemisphere Publishing.
- LIVINGSTONE, D. M. 1999. Ice break-up on southern Lake Baikal and its relationship to local and regional air temperatures in Siberia and to the North Atlantic Oscillation. *Limnol. Oceanogr.* **44**: 1486–1497.
- . 2003. Impact of secular climate change on the thermal structure of a large temperate central European lake. *Clim. Change* **57**: 205–225.
- , AND M. T. DOKULIL. 2001. Eighty years of spatially coherent Austrian lake surface temperatures and their relationship to regional air temperature and the North Atlantic Oscillation. *Limnol. Oceanogr.* **46**: 1058–1066.
- MANTUA, N. J., AND S. R. HARE. 2002. The Pacific decadal oscillation. *J. Oceanogr.* **58**: 35–44.
- , ———, Y. ZHANG, J. M. WALLACE, AND R. C. FRANCIS. 1997. A Pacific interdecadal climate oscillation with impacts on salmon production. *Bull. Am. Meteorol. Soc.* **78**: 1069–1079.
- MAZUMDER, A., AND W. D. TAYLOR. 1994. Thermal structure of lakes varying in size and water clarity. *Limnol. Oceanogr.* **39**: 968–976.
- MCCORMICK, M. J., AND G. L. FAHNENSTIEL. 1999. Recent climatic trends in nearshore water temperatures in the St. Lawrence Great Lakes. *Limnol. Oceanogr.* **44**: 530–540.
- MCGABE, G. J., AND M. D. DETTINGER. 1999. Decadal variations in the strength of ENSO teleconnections with precipitation in the western United States. *Int. J. Climatol.* **19**: 1399–1410.
- MCGOWAN, J. A., D. R. CAYAN, AND L. M. DORMAN. 1998. Climate-ocean variability and ecosystem response in the northeast Pacific. *Science* **281**: 210–217.
- MELACK, J. M., J. DOZIER, C. R. GOLDMAN, D. GREENLAND, A. M. MILNER, AND R. J. NAIMAN. 1997. Effects of climate change on inland waters of the Pacific coastal mountains and western great basin of North America. *Hydrol. Process.* **11**: 971–992.
- NATIONAL RESEARCH COUNCIL. 2002. *Scientific evaluation of biological opinions on endangered and threatened fishes in the Klamath River Basin: Interim report*. National Research Council.
- OVERLAND, J. E., AND R. W. PREISENDORFER. 1982. A significance test for principal components applied to a cyclone climatology. *Monit. Weather Rev.* **110**: 1–4.
- PEETERS, F., D. M. LIVINGSTONE, G. GOUDSMIT, R. KIPFER, AND R. FORSTER. 2002. Modeling 50 years of historical temperature profiles in a large central European lake. *Limnol. Oceanogr.* **47**: 186–197.
- POST, E., N. C. STENSETH, R. LANGVATN, AND J. M. FROMENTIN. 1997. Global climate change and phenotypic variation among red deer cohorts. *Proc. R. Soc. Lond. B. Biol.* **264**: 1317–1324.
- QUAY, P. D., W. S. BROECKER, R. H. HESSLEIN, AND D. W. SCHINDLER. 1980. Vertical diffusion rates determined by Tritium tracer experiments in the thermocline and hypolimnion of two lakes. *Limnol. Oceanogr.* **25**: 201–218.
- QUINN, T. P., S. HODGSON, AND C. PEVEN. 1997. Temperature, flow, and the migration of adult sockeye salmon (*Oncorhynchus nerka*) in the Columbia River. *Can. J. Fish. Aquat. Sci.* **54**: 1349–1360.
- RICHMAN, M. B. 1986. Rotation of principal components. *J. Climatol.* **6**: 293–335.
- ROEMMICH, D., AND J. MCGOWAN. 1995. Climatic warming and the

- decline of zooplankton in the California current. *Science* **267**: 1324–1326.
- SCHINDLER, D. W., AND OTHERS. 1996. The effects of climatic warming on the properties of boreal lakes and streams at the Experimental Lakes Area, northwestern Ontario. *Limnol. Oceanogr.* **41**: 1004–1017.
- , AND OTHERS. 1990. Effects of climatic warming on lakes of the central boreal forest. *Science* **250**: 967–970.
- SHUTER, B. J., D. A. SCHLESINGER, AND A. P. ZIMMERMAN. 1983. Empirical predictors of annual surface water temperature cycles in North American lakes. *Can. J. Fish. Aquat. Sci.* **40**: 1838–1845.
- STRAILE, D. 2000. Meteorological forcing of plankton dynamics in a large and deep continental European lake. *Oecologia* **122**: 44–50.
- STRUB, P. T., T. POWELL, AND C. R. GOLDMAN. 1985. Climatic forcing: Effects of El Niño on a small temperate lake. *Science* **227**: 55–57.
- WALTERS, R. A. 1980. Time and depth-dependent model for physical, chemical and biological cycles in temperate lakes. *Ecol. Model.* **8**: 79–96.
- WEYHENMEYER, G., A. T. BLENCKER, AND K. PETTERSSON. 1999. Changes of the plankton spring outburst related to the North Atlantic Oscillation. *Limnol. Oceanogr.* **44**: 1788–1792.
- WILLMOTT, C. J., AND K. MATSUURA. 2000. Terrestrial air temperature and precipitation: Monthly and annual time series (1950–1996). http://climate.geog.udel.edu/~climate/html-pages/README_ghcn_ts.html
- WOLTER, K., AND M. S. TIMLIN. 1993. Monitoring ENSO in COADS with a seasonally adjusted principal component index, p. 52–57. *In* Proceedings of the 17th Climate Diagnostic Workshop, Norman, OK. NOAA/NMC/CAC, NSSL, Oklahoma Climate Survey, CIMMS and the School of Meteorology, Univ. Oklahoma.
- ZHANG, Y., J. M. WALLACE, AND D. S. BATTISTI. 1997. ENSO-like interdecadal variability: 1900–93. *J. Climate* **10**, 1004–1020.

Received: 22 October 2002

Accepted: 12 August 2003

Amended: 3 September 2003